

Characterization of mechanical properties of a Zr-based metallic glass by indentation techniques

Chunguang Tang^{a,b}, Yi Li^b, Kaiyang Zeng^{a,*}

^a Institute of Materials Research and Engineering, 3 Research Link, Singapore 117602, Singapore

^b Department of Materials Science, National University of Singapore, 10, Lower Kent Ridge Crescent, Singapore 119620, Singapore

Received 19 December 2003; received in revised form 25 May 2004

Abstract

This paper presents studies on mechanical properties of a Zr-based metallic glass by using spherical indentation and nano-indentation techniques. The spherical indentation investigates mechanical properties of the Zr-based metallic glass as a function of indentation strain. The results show that the Zr-based metallic glasses have almost perfect plasticity with little strain hardening. During fully plastic stage, spiral shear bands appear inhomogeneously around the impression of the spherical indentations. The shear bands initiate from the impressions at an angle slightly deviating from the pure shear stresses in the free surface. Further nano-indentations by using Berkovich tip made around the spherical indentation impression show that there is a zone of lower hardness around the impression of the spherical indentation. SEM and AFM images show that there exists significant different pile-up behaviors of the impressions by the nano-indentation far away and near the spherical indentation impression. Near the spherical indent, less pile-up is formed around the impression of nano-indentation, and this is assumed to be the result of the intersection between the pre-introduced shear bands by the spherical indentation and the new shear bands induced by nano-indentation.

© 2004 Elsevier B.V. All rights reserved.

Keywords: Metallic glass; Mechanical properties; Shear band; Spherical indentation; Nano-indentation

1. Introduction

Bulk metallic glass (BMG) can exhibit either inhomogeneous or homogeneous mechanical behavior [1], depending on the environmental temperature and stress state. At high temperature and low stress, especially in the supercooled liquid region, metallic glass shows a homogeneous mechanical behavior and exhibits significant plasticity. While at room temperature (T_r) and high stress, inhomogeneous, severely localized shear bands occur. These bands can result in a rapid band propagation and catastrophic failure under tensile stress, revealing no evidence of macroscopic plasticity [2].

Indentation experiment, traditionally as a hardness testing method, can introduce a constrained or stable stress field and thus provides a way to characterize multiaxial plastic deformation of bulk metallic glass at T_r . Much work has been done to investigate the mechanical behavior of bulk metallic glasses through sharp indentation

[3–5]. For example, Vaidyanathan et al. [3] have conducted Berkovich indentations and finite element simulations on $Zr_{41.25}Ti_{13.75}Cu_{12.5}Ni_{10}Be_{22.5}$ and found that normal stress sensitive Mohr-Coulomb yield criterion can be applied to this material. Kim et al. [4] have also conducted Berkovich nano-indentation on $Zr_{52.5}Cu_{17.9}Ni_{14.6}Al_{10}Ti_5$ at room temperature and explored the shear bands by using of transmission electron microscopy. They found that nanocrystallites nucleate in and around shear bands produced near indents and these nanocrystallites are the same as those formed during annealing without deformation. They attributed the nanocrystallites to the high atomic mobilities caused by flow dilatation in the shear bands. Schuh and Nieh [5] have conducted nano-indentations on Pd- and Zr-based bulk metallic glasses with loading rates from 0.02 to 300 mN/s. They found that stepped load-displacement curves, corresponding to the serrated flow during nano-indentations, occurred at very low loading rates. At high loading rates, the serrated flow was completely suppressed. They attributed these results to the kinetic limitation for shear bands. When the applied loading rate is low, a single shear band can

* Corresponding author.

E-mail address: ky-zeng@imre.a-star.edu.sg (K. Zeng).

rapidly accommodate the deformation and thus serrated flow occurs. In contrast, when the loading rate exceeds the rate of relaxation by a single shear band, multiple shear bands have to operate simultaneously and lead to smooth load-displacement curves.

Most of the studies on indentation behaviour of BMG have been using sharp indenter tip, i.e., pyramidal or conical tips. Due to the geometrical similarity, the indentation strain produced by sharp indenter remains a constant during indentation, independent of the applied load [6]. It is therefore difficult to provide information of BMG mechanical behaviour at different strain stages by using the sharp indenter tips. While for the indentations with the spherical tips, the indentation strain increases with the load applied to the indenter. This gives the possibility to study the mechanical properties as the function of the indentation strain. In this paper, we therefore explore the mechanical behaviour of a Zr-based bulk metallic glass based on spherical indentation and nano-indentation techniques.

2. Theory of spherical indentation

The deformation of metals under spherical indentation normally experiences three stages [7,8], which can be distinguished by the parameter defined as P_m/Y , where P_m is the mean pressure in indentation and Y is the flow stress of metals. When $P_m/Y < 1.1$, the deformation is fully elastic. As soon as P_m/Y reaches 1.1, plasticity initiates at the point of maximum shear stress beneath the centre of contact circle. As the load increases in the material, mean pressure P_m raises and the plastic zone expands. At this stage, for an elastic-perfectly plastic material, the flow stress keeps as a constant, while for elastic-plastic material; the flow stress increases to Y_ϵ , which corresponds to the strain ϵ at that load. As the indentation load increases further, the plastic zone expands to the free surface of the material and the whole material around the indenter is in a plastic status. At this point, P_m/Y or $P_m/Y_\epsilon \cong 3$, full plasticity is reached. If the load increases further, for elastic-plastic material the ratio of P_m/Y_ϵ remains approximately constant with both P_m and Y_ϵ increasing till P_m reaches the ultimate hardness; while for elastic-perfectly plastic material, P_m keeps almost constant.

Meyer [9] found that for various metals under indentation with a ball of fixed diameter D , the indentation load P , and diameter of contact, d (Fig. 1), have following relation

$$P = Kd^n \quad (1)$$

where K and n are material constants. n is called Meyer index and usually has the value between 2 and 2.5. For fully annealed metals, n is near 2.5; and for fully work-hardened metals it is around 2. This relation is considered valid to the point of $d/D \cong 1$, that is, the penetration depth is almost the same as the radius of the ball indenter. However, there is a lower limit to this equation. Meyer found that this lower limit is $d/D = 0.1$, where full plasticity is developed.

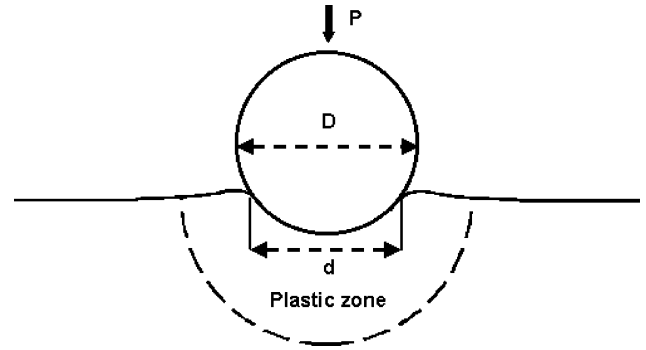


Fig. 1. Schematic drawing of spherical indentation.

At very low load, metals deform elastically and n increase towards 3. Later, Tabor [9] proposed that the lower limit of Meyer's law depends on the hardness of the metal under indentation. Based on finite element investigations [10], Herbert et al. have proposed that this lower limit should be at $d/D \cong 0.16$ [11].

Assuming that the yield stress is a simple power function of strain, Tabor [12] deduced the relationship between Meyer's index n and the strain-hardening index x as follows:

$$n = 2 + x \quad (2)$$

To investigate the mechanical behaviours of metallic glasses under spherical indentation, it is helpful to understand the stress distribution around the indenter. The contact between a hard spherical indenter and a flat surface is a special case of the well-known Hertz contact. In Hertzian stress field, there are three principal stresses [13]: radial stress σ_1 , hoop stress σ_2 and the stress along load axis, σ_3 . At the surface inside the contact circle, all the principal stress are compressive and $\sigma_1 > \sigma_2 > \sigma_3$. This relationship is valid for most of the contact area. In the free surface outside the contact circle, however, the stress field is quite different (Fig. 2). σ_1 becomes tensile and σ_2 remains compressive, of which the magnitudes are the same and decrease with radial distance. The radial stress, σ_1 is mainly responsible

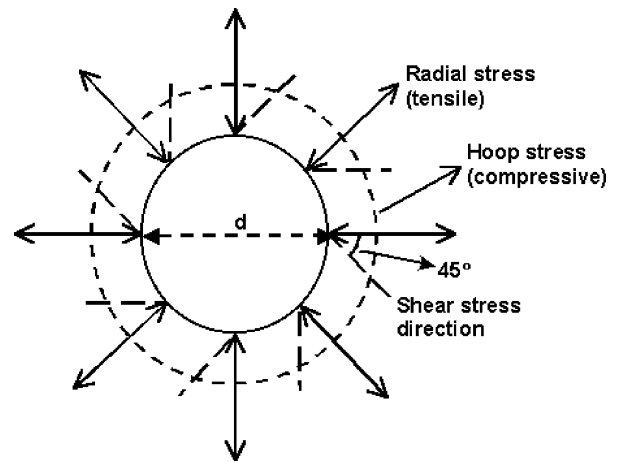


Fig. 2. Schematic drawing showing stress distribution in the free surface around spherical indent.

for the crack initiation and the hoop stress, σ_2 , expands it into a ring crack. σ_3 drops to zero. This is an indication that the stress outside the contact circle is under pure shear stress at 45° to the radial direction.

3. Materials and indentation experiments

Bulk metallic glass Zr–5Ti–17.9Cu–14.6Ni–10Al (wt.%) (vit105) was prepared by arc melting the pure elements under a Ti-gettered Ar atmosphere, followed by casting in a water-cooled copper mould. The resulting ingot dimensions were $1.6 \text{ mm} \times 5 \text{ mm} \times 30 \text{ mm}$. The morphology of the material was examined by using X-ray diffraction (XRD, Gadds XRD system, Bruker, USA) with Cu $K\alpha$ radiation.

The as-cast samples were mechanically polished to mirror smooth and then indented by a spherical diamond indenter tip with a nominal radius of $200 \mu\text{m}$ (Gilmore Diamond Tools, RI, USA). A series of indentations with loads from 10 to 240 N at displacement rate of 0.1 mm/min were conducted using Instron Micro-force Tester (Instron Ltd., USA). The dimensions of the residual indents were measured using optical microscope immediately after indentation. Fracture strength of the as-cast vit105 was also determined through un-constraint compression test, the specimens had dimension of $1.5 \text{ mm} \times 1.5 \text{ mm} \times 3 \text{ mm}$, the tests were done with the strain rate of 10^{-4} using the Instron Servo-hydraulics universal test machine.

To investigate the effects of the residual plastic strain due to spherical indentation on the material, nano-indentations were conducted using a standard Berkovich indenter tip on a Nano-indenter (UMIS-2000H, CSIRO, Australia) at 40 mN on the free surface radially outwards with spacing of $20 \mu\text{m}$ in 12 symmetrical directions. The nano-indentations were placed from 20 to $240 \mu\text{m}$ away from the spherical indent edge. The nano-indentations were further examined under Scanning Electron microscopy (SEM, JEOL 6700F, JEOL Ltd., Japan) and Atomic Force Microscopy (AFM, MultiMode[®], Veeco, USA) to study the deformation patterns around the indentations.

4. Results and discussion

4.1. Morphology of vit105

The XRD measurement of the as-cast vit105 showed that there was no evidence of crystalline structures in the material. Further, Differential Scanning Calorimeter (DSC, DSC 2900, TA Instruments, USA) measurement at a heating rate of 10 K/min showed several crystallization peaks upon heating up to 873 K . These results indicated that the vit105 had amorphous structure at room temperature, whereas crystallization occurred only at the high temperature. These results were in good agreement with the results for this alloy reported in the literature [14,15].

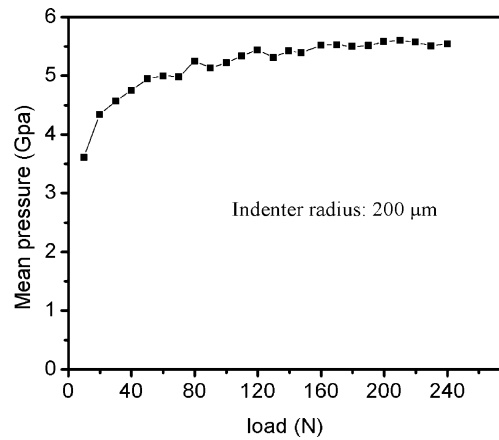


Fig. 3. Mean pressure vs. indentation load for metallic glass vit105 obtained by spherical indentation using a indenter with radius of $200 \mu\text{m}$.

4.2. Spherical indentations

Fig. 3 showed the relationship between the indentation mean pressures and the indentation load resulting from the spherical indentation with the indenter radius of $200 \mu\text{m}$. The mean pressure was defined as $p_{\text{ave}} = P/A$, whereas A was the contact area measured after indentation by using optical microscope. The mean pressure increased with increasing load until it reached to about 5.5 GPa at the load of 160 N . After that, the mean pressure is kept as almost constant upon further increasing of the indentation loads. The average mean pressure value was slightly lower than the hardness obtained using nano-indentation reported in the literature [15]. We believed that this difference was due to the material pile-up around the nano-indentation, which was an important factor influencing the results of nano-indentation and would be discussed below.

The relationship between P and d for vit105 was shown as a plot of $\log(P)$ versus $\log(d)$ in Fig. 4. As shown in the figure, the initial stage of the curve had a slope of about

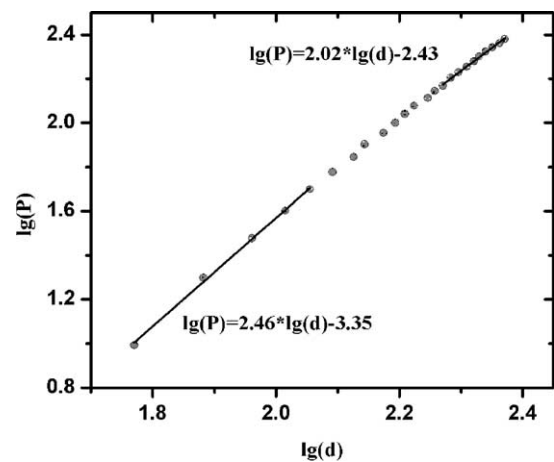


Fig. 4. Relations between $\log(P)$ and $\log(d)$ to reveal the values of n in Eq. (1).

2.5. Since at the elastic stage during spherical indentation, the value of n should be near to 3, the present result suggested that even at load as small as 10 N, plastic deformation most likely already took place beneath the spherical indent. As the load increased further, the slope decreased and approached to 2 when the load increased to more than 150 N. According to Eq. (2), this indicated that the strain-hardening index x was about 0 at this stage, meaning no strain hardening in this material, which agreed with the characteristics of elastic-perfect plastic properties of the metallic glasses.

4.3. Yielding stress determined from indentation

Yielding stress of the vit105 could be determined based on the indentation experiments since the vit105 showed elastic-perfect plastic properties, Tabor has built an empirical model that for ideally plastic metals, the hardness and yield stress had relationship $H/Y = 2.8$ [9]. According to this empirical model, vit105 should have a yielding strength of about 1.96 GPa when the constant mean pressure (5.5 GPa) in Fig. 3 is taken to be the value of hardness. The values of hardness and yielding stress were consistent with those measured on another Zr-based alloy, Vitreloy 1 ($Zr_{40}Ti_{14}Ni_{10}Cu_{12}B_{24}$) [16,17]. This yielding stress was higher than the fracture strength of the vit105 determined from the un-constraint compression test. The fracture strength from the compressive test was 1.7 GPa without apparent plastic deformation. This compressive fracture strength was lower than that reported in the literature for most of metallic glasses, it might be due to that the compressive tests were performed with unconstraint condition in

which might lower the strength. The lack of apparent plastic deformation indicated that compression failure took place most likely before yielding and the yielding stress should be higher than 1.7 GPa for vit105. If we assumed the yielding stress of the vit105 to be in the range of 1.7–1.96 GPa, then we found that the ratio of H/Y were about 3.3–2.8. This result was in agreement with what observed by Davis [18] on $Ni_{49}Fe_{29}P_{14}B_6Si_2$ and $Pd_{77.5}Cu_6Si_{16.5}$ metallic glasses in which the H/Y ratios for both alloys were to be around 3.2.

4.4. Deformation during indentation

When the load increased further to more than 200 N during the spherical indentation, shear bands were found around the indentation impressions. The features of the shear bands at the load of 230 N were shown in Fig. 5. The shear bands originated from the periphery of residual impression and moved outwards in the direction of the shear stresses on the free surface. The shear bands were not straight, but were spiral in shape. This was because along the shear bands, the directions of the radial, hoop and thus shear stresses were constantly changing in a spiral fashion (see Fig. 2). Such spiral shear bands had been found around spherical indentation on nanocrystalline iron using an automated ball indentation technique [19]. It was determined that the shear bands emerged from the indentation at an angle of about 45° and met each other at an angle of about 90° [19]. In the present work, however, careful measurement revealed that angles between the shear bands were about 80° near the indent edge (Fig. 6). Since on the free surface around the spherical indent, the stresses were pure shear and along 45° to the

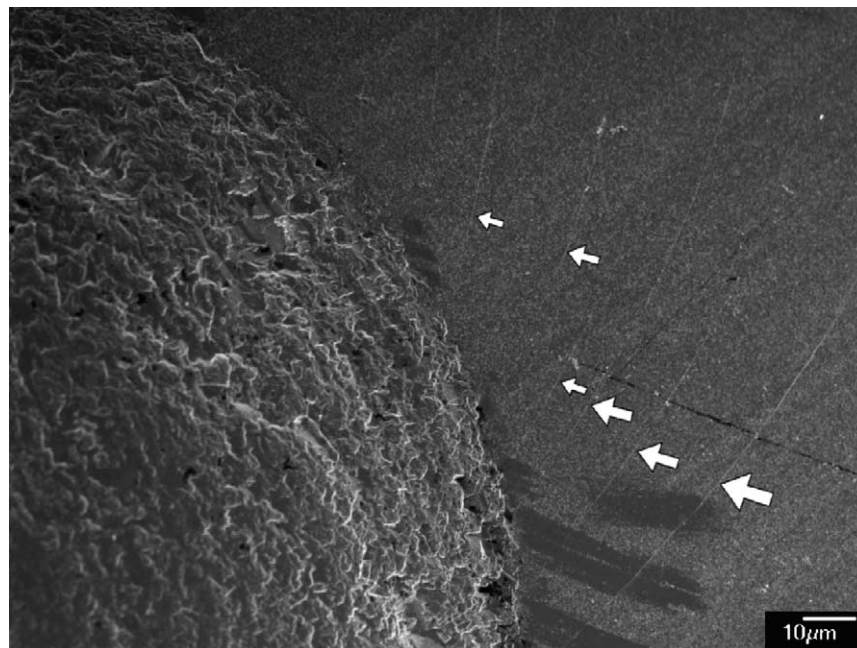


Fig. 5. Morphology for spherical indent on metallic glass vit105 at load of 280 N. Arrows indicated the shear bands due to the spherical indentation. The indent was located in the left side of the picture.

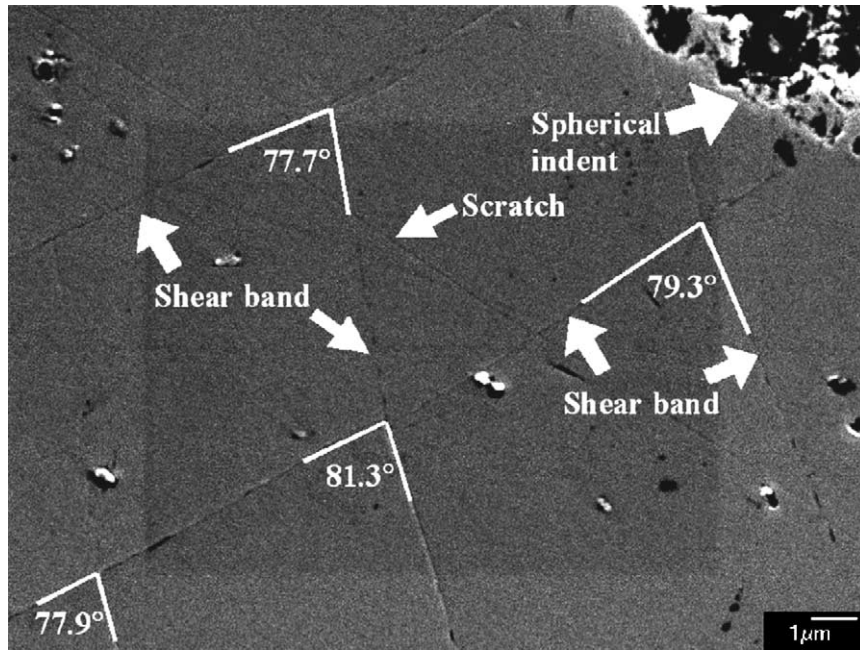


Fig. 6. Angles between shear bands nearby spherical indent edge revealed the influence of normal stress on the plastic deformation of metallic glasses.

radii near the indent, which translated into an angle of 90° between the pronged shear bands. The angles in our work was different from 90° indicated that the shear band did not follow the maximum shear stress. Many works on metallic glasses have noted that the shear bands in several metallic glasses did not appear to be associated with the plane of maximum shear stress, hence accordingly does not follow the von Mises criterion [17,20]. Danavan [21,22] has proposed that the metallic glasses followed the Mohr-Coulomb yielding criterion, in which could be used to predict shear band orientation. Our results presented here were also consistent with those reported about shear band orientation [17,20–22].

At the room temperature, the catastrophic failure of metallic glasses in tensile tests made the stress-strain curve similar to that of brittle materials [2]. To compare the spherical indentation behaviours between metallic glasses and brittle materials, we also performed spherical indentation on soda-lime glass. The indentation at a load of 33 N introduced ring cracks around the contact circle, which were representative characteristics of brittle materials subjected to spherical indentation [13,23]. The ring cracks indicated that the behaviours of brittle materials are dominated by principal stresses, not shear stresses as in the metallic glasses.

4.5. Nano-indentations around spherical indentation site

Fig. 7 schematically showed the general pattern of the nano-indentations made around the spherical indent. Fig. 8 showed the averaged hardness values in the free surface measured by nano-indentation as a function of the distance from the edge of the spherical indent at the load of 230 N. The hardness values from nano-indentation experiments were de-

termined by using Oliver and Pharr’s analysis [24]. At this load, the material beneath the spherical indent was fully plastic and the contact circle had a radius of about $110 \mu\text{m}$. Fig. 8 revealed that, compared to the area near the spherical indent, the area far away had higher hardness. In the lower hardness zone, the hardness decreased further if the indent by nano-indentation approached to the edge of the spherical indent.

This phenomenon was quite different from that reported for the crystalline metals. Tabor [12] measured the Vickers

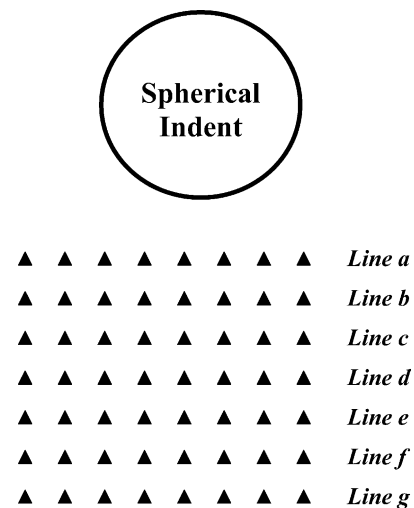


Fig. 7. Schematically drawing of the patterns of Berkovich nano-indentations around a spherical indentation impression, nano-indentations were made of several lines in the lateral direction of the spherical indents: lines a and b were in the pre-introduced shear bands zone near the spherical indent; lines f and g were beyond the zone.

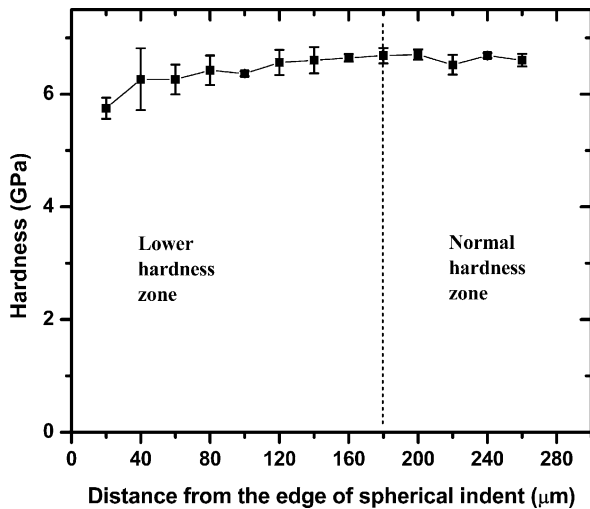


Fig. 8. Hardness measured by nano-indentation around a spherical indent with radius of 110 μm on metallic glass vit105.

hardness on the free surface around the spherical indentation impression of various sizes (d/D) formed in mild steel. He found that outside the spherical impression, the Vickers hardness increased by more than 400 MPa when approached to the edge of impression. Later, Williams and O'Neill [25] made surface and sectional explorations in annealed copper subjected to spherical indentation of various sizes (d/D). They found that the zone around indentation had higher hardness and that larger spherical indentation size led to a greater increase to the hardness around it.

In order to determine the reasons of the apparent softening around the spherical indent in metallic glasses, we selected some typical indents in both the softened and the normal zone for details study. SEM and AFM images for the indent in the lines (a), (d) and (g) (see Fig. 7 for detail), were shown in Fig. 9(a)–(f). The indents in the line (a) were within the zone of the pre-introduced shear bands, the indents in the line (d) were at the boundary of the pre-introduced shear bands, and the indents in the line (g) were in the normal zone where no pre-introduced shear bands. It is revealed that for the nano-indentations made from line (a) to line (d) and further to line (g), the side lengths of nano-indentations, or the “apparent” projected contact area was kept decreasing. In the nano-indentation, these apparent contact areas were used to calculate the hardness. It was clear that the increase in the apparent contact area was responsible for the apparent decrease of hardness in the softened zone. However, in the softened zone, almost no or only small pile-up around the nano-indentation impression could be found (Fig. 9(a–d)), while in the normal zone, large pile-up was found around the nano-indentation impressions. On one side of the nano-indentation impression that was located in the normal zone, the pile-up even extended to the corners (Fig. 9(e, f)).

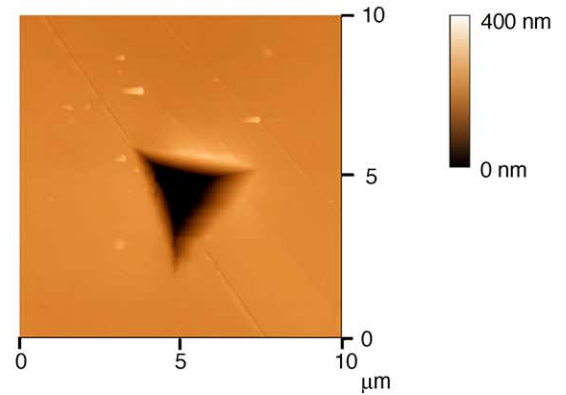
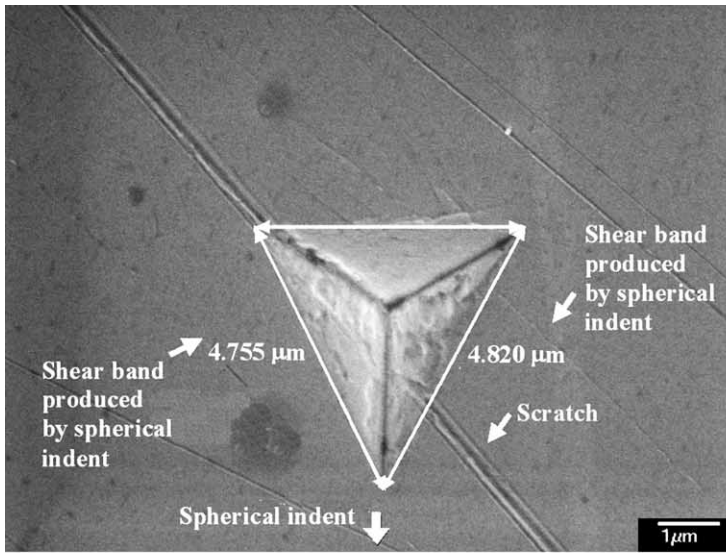
Pile-up was an important factor influencing the results and analysis of the nano-indentation tests, during which the

(projected) contact area was deduced from the indentation depth. By applying controlled stresses by bending the specimen, Tsui et al. [26] investigated the influences of applied stress on the measurement of hardness by nano-indentation. They found that the conventional observation of dependence of hardness on residual stress state is due to the error in contact area calculation arising from pile-up. After taking pile-up into account, they found that residual stress did not affect the hardness measured from nano-indentation.

In the present work, it was clear that the pile-up around the nano-indentation impressions diminished in approach to the spherical indent. We believed that the influence by residual stresses could not fully explain the phenomenon here as the metallic glass deforms elastically outside the shear bands and the stresses were released after the spherical indentation load is removed.

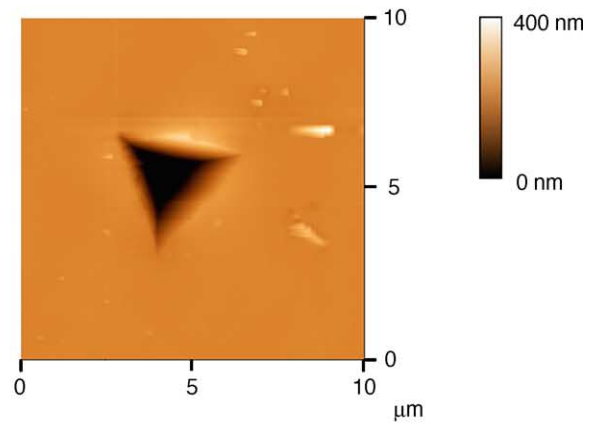
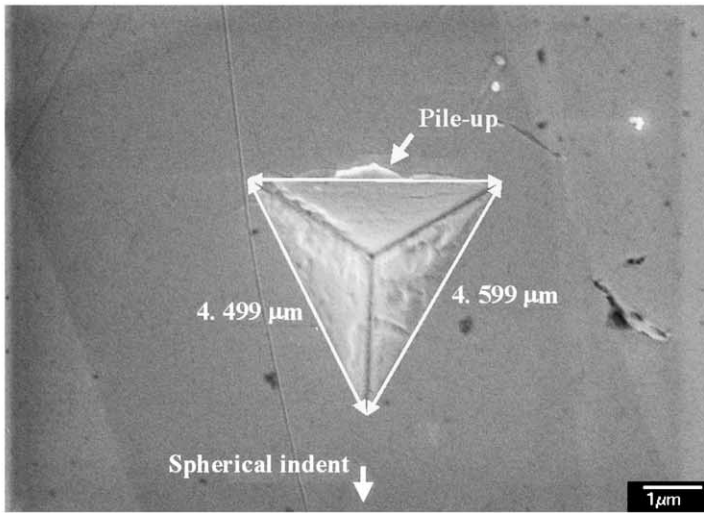
Takayama [27] had investigated the drawing behavior of $\text{Pd}_{77.5}\text{Cu}_6\text{Si}_{16.5}$ metallic glass wires and found that the plastic flow within the shear bands at the exit of the die did not continue and result in fracture owing to work softening. He proposed that this was due to the anti-action of work hardening resulting from the intersection of shear bands, which stopped the further movement of shear bands. He also observed terminations of shear bands by other bands. After drawing, the specimen with such pre-existing shear bands exhibited more elongation and slightly higher fracture stress during tension tests. Later on, Hagiwara et al. [28] observed similar phenomena in drawn wire of metallic glass $\text{Co}_{72.5}\text{Si}_{12.5}\text{B}_{15}$. They studied the tensile strength and the fracture elongation for this alloy with various cold-drawn reductions in area and found that the strength and elongation increased till the area reduction reached about 60 and 30%, respectively. On the bending samples after cold drawing to 41% reduction, they also detected that a large number of shear bands intersected each other and others terminated some. Kimura and Masumoto [2] attributed the enhanced elongation to local yielding in the pre-existing shear bands and the higher fracture stress to the intersection of shear bands. However, it should be noticed that, as pointed out by Kimura and Masumoto [2], such work hardening was not intrinsic (physical) strain hardening, since an individual shear band was of an ideal-plastic nature and the material outside the shear band possesses no plastic strain. It was of interest to note that such situation seldom occurred in metallic glasses subjected to uniaxial loading such as tension and compression tests, where shear bands did not intersect with each other. This suggested that this phenomenon is dominated by the intersection of the shears bands due to the different stress states.

During the indentation, pile-up usually took place in ideally plastic materials and sink-in occurred in strain-hardening materials. For ideally plastic materials, the part near the indenter was stressed and moves upwards around the indenter, forming pile-up. For strain-hardening materials, the most stressed part near the indenter was hardened and moves downwards along with the indenter, forming sink-in.



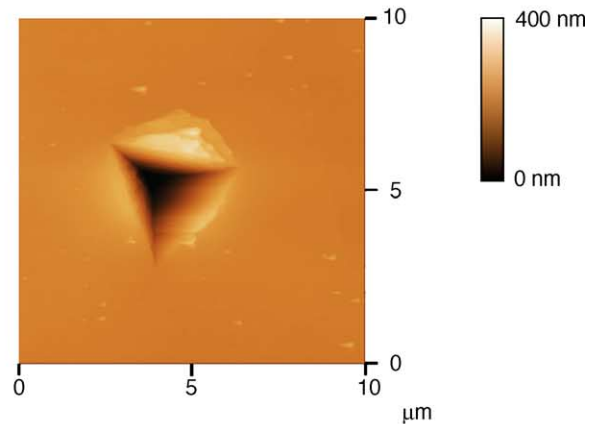
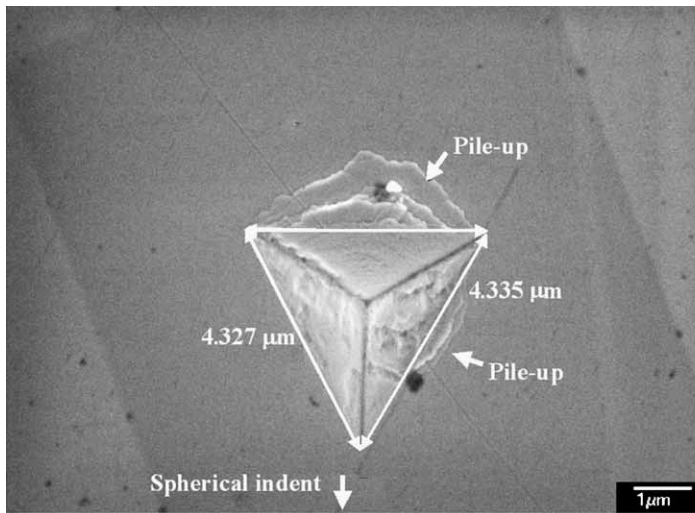
(a)

(b)



(c)

(d)



(e)

(f)

Fig. 9. SEM and AFM images for Berkovich nano indents around spherical indent with radius of 110 μm . (a, b) The first indent; (c, d) the fourth indent; (e, f) the seventh indent.

In this case, the material far away from the indenter could move both upwards and outwards. In our work, the metallic glass far away from the spherical indentation impression showed obvious pile-up during nano-indentation, exhibiting ideal plasticity. However, because of ideally plasticity of metallic glasses, the disappearance of pile-up around nano-indentation near the spherical indentation impression could not be explained by the concept of strain hardening. Since the pile-up (or plastic deformation) of metallic glasses took place through shear band movement, we believed that the pile-up disappearance is due to the intersection between the pre-existing shear bands (by spherical indentation) and the new shear bands (by nano-indentation). This result was similar to that presented by Gilbert et al. [29], in which they indicated that the shear bands did cut through each other. A possible explanation for this phenomenon was that the plastic flow surrounding the nano-indentations near the spherical indentation was somewhat accommodated by the reactivation of the pre-existing shear bands. It has been suggested that the shear bands were regions of higher free volume [30], therefore it was reasonable to assume that this region would be weaker than the surrounding material and more prone to additional deformation. These moving shear bands also inhibited the motion of the new shear bands and for the pile-up around nano-indentation to occur. Another possible reason for the less pile-up in the region of near the spherical indents could be due to the possible effects of densification under the nano-indentation sites. Since the pre-existing shear bands had higher free volume than surrounding materials [30], then this region would have a lower density, therefore if the material became more dense due to the indentation, then there would be less pile-up around the indentation edges.

Schuh and Nieh [5] have studied the serrated flow of metallic glasses using nano-indentation. They found that at high strain rates, many shear bands move at the same time to accommodate the strain and thus the nano-indentation P – h (load–displacement) curves were smooth, while at low strain rates, only a few shear bands move and thus the P – h curves were serrated. On top of their results, it was reasonable to expect a more serrated P – h curve during nano-indentation at constant strain rates for metallic glass in which the movement of shear bands was suppressed. We conducted further nano-indentations at a constant strain rate around the spherical indentation impression, and found that the nano-indentations far away had relatively smooth P – h curves, while those near the spherical indentation impression resulted in quite serrated P – h curves. These results further supported the analysis provided previously and will be presented and discussed separately.

5. Summary

Plastic deformation behavior and mechanical properties of metallic glass vit105 are investigated by using spheri-

cal indentation and nano-indentation experiments. We find that spherical indentation is a good method to study the mechanical properties of the metallic glass as the function of indentation strain. The results show that metallic glasses have constant hardness upon indentation strain increases to a fully plastic stage, showing the ideal plasticity of metallic glasses. It is found that the vit105 has hardness of 5.5 GPa and yielding stress of 1.96 GPa by using spherical indentation. These results are consistent with others reported in the literature. During the fully plastic stage, spiral-like shear bands appear around the spherical indent, indicating that the plastic deformation of the metallic glass is dominated by shear stresses. The slight deviation of shear bands from the direction of pure shear stresses in the free surface reveals the influence of stresses within the interior of specimen on the propagation of shear bands. Within close vicinity of the spherical indent, Berkovich nano-indentations introduce little pile-up. This is most likely due to the intersection between the pre-introduced shear bands produced by spherical indentation and the new shear bands by nano-indentation, which can suppress the new shear bands and thus the pile-up around the nano-indentation.

Acknowledgements

The authors would like to thank Ms. Lu Shen and Ms. Joyce Tan for their help during indentation experiments and Ms. Lee Mei Ling Irene for valuable discussion during the course of this work.

References

- [1] F. Spaepen, A.I. Taub, in: F.E. Luborsky (Ed.), *Amorphous Metallic Alloys*, Butterworth & Co. (Publishers) Ltd., 1983 (Chapter 13).
- [2] H. Kimura, T. Masumoto, in: F.E. Luborsky (Ed.), *Amorphous Metallic Alloys*, Butterworth & Co. (Publishers) Ltd., 1983 (Chapter 12).
- [3] R. Vaidyanathan, M. Dao, G. Ravichandran, S. Suresh, *Acta Mater.* 49 (2001) 3781.
- [4] J.-J. Kim, Y. Choi, S. Suresh, A.S. Argon, *Science* 295 (2002) 654.
- [5] C.A. Schuh, T.G. Nieh, *Acta Mater.* 51 (2003) 87.
- [6] A.C. Fischer-Cripps, *Nano-indentation*, Springer-Verlag New York Inc., 2002.
- [7] D. Tabor, *The Hardness of Metals*, Oxford University Press, London, UK, 1951 (Chapter 4).
- [8] J.S. Field, M.V. Swain, *J. Mater. Res.* 10 (1995) 101.
- [9] D. Tabor, *The Hardness of Metals*, Oxford University Press, London, UK, 1951 (Chapter 2).
- [10] S.D. Mesarovic, N.A. Fleck, *Proc. R. Soc. Lond. A* 455 (1999) 2707.
- [11] E.G. Herbert, G.M. Pharr, W.C. Oliver, B.N. Lucas, J.L. Hay, *Thin Solid Films* 398/399 (2001) 331.
- [12] D. Tabor, *The Hardness of Metals*, Oxford University Press, London, UK, 1951 (Chapter 5).
- [13] B.R. Lawn, *J. Appl. Phys.* 39 (1968) 4828.
- [14] T.C. Hufnagel, X.F. Gu, A. Munkholm, *Mater. Trans. JIM* 42 (2001) 562.
- [15] J.G. Wang, B.W. Choi, T.G. Nieh, C.T. Liu, *J. Mater. Res.* 15 (2000) 798.

- [16] H.A. Bruck, T. Christman, A.J. Rosakis, W.L. Johnson, *Scripta Mater.* 30 (1994) 429.
- [17] W.J. Wright, R. Saha, W.D. Nix, *Mater. Trans. JIM* 42 (2001) 642.
- [18] L.A. Davis, *Scripta Metall.* 9 (1975) 431.
- [19] T.R. Malow, C.C. Koch, P.Q. Miraglia, K.L. Murty, *Mater. Sci. Eng. A* 252 (1998) 36.
- [20] Z.F. Zhang, J. Eckert, L. Schultz, *Acta Mater.* 51 (2003) 1167.
- [21] P.E. Donovan, *Mater. Sci. Eng.* 98 (1988) 487.
- [22] P.E. Donovan, *Acta Mater.* 37 (1989) 445.
- [23] K. Zeng, K. Breder, D.J. Rowcliffe, *Acta Metall. Mater.* 40 (1992) 2601.
- [24] W.C. Oliver, G.M. Pharr, *J. Mater. Res.* 7 (1992) 1564.
- [25] H. O'Neill, *Hardness Measurement of Metals and Alloys*, The Thanet Press, Margate, 1967 (Chapter 3).
- [26] T.Y. Tsui, W.C. Oliver, G.M. Pharr, *J. Mater. Res.* 11 (1996) 752.
- [27] S. Takayama, *Mater. Sci. Eng.* 38 (1979) 41.
- [28] M. Hagiwara, A. Inoue, T. Masumoto, *Mater. Sci. Eng.* 54 (1982) 197.
- [29] C.J. Gilbert, V. Schroeder, R.O. Ritchie, *Metall. Mater. Trans. A* 30A (1999) 1739.
- [30] K.M. Flores, D. Suh, R.H. Danskardt, *J. Mater. Res.* 17 (2002) 1153.